



PERGAMON

Atmospheric Environment 36 (2002) 1863–1874

ATMOSPHERIC  
ENVIRONMENT

www.elsevier.com/locate/atmosenv

# Modeling the number distributions of urban and regional aerosols: theoretical foundations

K. Max Zhang\*, Anthony S. Wexler

*Department of Mechanical and Aeronautical Engineering, University of California, Davis, CA 95616, USA*

Received 10 September 2001; received in revised form 19 December 2001; accepted 4 January 2002

## Abstract

Recent studies suggest an association between particle number concentrations and adverse health effects in humans and laboratory animals. A photochemical model able to predict the particle number distribution and concentration will be very helpful to establish the association between emissions and air quality needed for developing rational emission control strategies. As the first step of the study, each term in the aerosol dynamic equation, namely condensation and evaporation, coagulation, gravitational settling, nucleation, advection, turbulent transport, emission, deposition and heterogeneous chemical reaction, is analyzed to estimate its influence on the overall number distributions under typical urban conditions. © 2002 Elsevier Science Ltd. All rights reserved.

*Keywords:* Aerosol model; Aerosol number distribution; Aerosol size distribution; Kelvin effect

## 1. Introduction

Recent studies have shown an association between ultrafine particles and adverse health effects: studies on rodents demonstrate that ultrafine particles administered to the lung cause a greater inflammatory response than do larger particles, per given mass (Oberdorster, 2001); the health effects of the 5-day mean of the number of ultrafine particles were found to be larger than those of the mass of the fine particles and its effects on the peak expiratory flow (PEF) were stronger than those of  $PM_{10}$  (Peters et al., 1997). Given the extremely high number but low mass of particles in this size range, a better model of aerosol number distribution will predict the properties of particles more accurately even if mass or surface area concentrations of ultrafine particles are also important.

The study of number distribution can be traced back to the derivation of the general dynamic equation (Gelbard and Seinfeld, 1979), which originally was in the form of rate of change of  $n(D_p, t)$ , where  $n(D_p, t) dD_p$

is the number of particles per volume of air with diameters in the range  $[D_p, D_p + dD_p]$ . Significant work has been carried out on techniques for the numerical solution of the general dynamic equation (Pilinis et al., 1987). Pilinis and Seinfeld (1987a) gave a solution for the case in which the effect of coagulation was small relative to the other phenomena such as condensation and evaporation represented in the equation, but not small enough to be neglected.

After that, more attention was given to the mass distribution (Pilinis et al., 1987; Pilinis and Seinfeld, 1987b; Pilinis, 1990). Wexler et al. (1994) showed that the time scale for coagulation is too long to significantly influence particle mass distributions and that chemical reactions in or on aerosol particles are insignificant for typical ambient conditions as long as relative humidity is  $< 100\%$ . And in comparison to deposition and turbulent diffusion, gravitational settling can also be ignored for  $PM_{10}$  (Wexler et al., 1994). Homogeneous  $H_2SO_4$ – $H_2O$  nucleation was shown to be a significant generator of new particles where the aerosol loading is low and the gas concentration of  $SO_2$  is high, and can therefore significantly alter the aerosol number distribution (Wexler et al., 1994).

\*Corresponding author. Fax: +1-530-752-4158.

E-mail address: maxzhang@ucdavis.edu (K. Max Zhang).

Our goal in this paper is to follow the similar steps as those taken in Wexler et al. (1994), but focus on accurate and numerically efficient prediction of number distribution, especially in the ultrafine size range. Note that the processes important to mass distributions are not necessarily important to number distributions, and vice versa.

## 2. The general dynamic equation

In a Eulerian frame of reference, the general dynamic equation that describes the number distribution of an internal mixed aerosol over time is

$$\begin{aligned}
 & \frac{\partial n(D_p, x, t)}{\partial t} \text{ (local rate of change)} \\
 & + (\mathbf{V}(x, t) - V_s(D_p)\mathbf{k}) \cdot \nabla n(D_p, x, t) \\
 & \text{(spatial advection and gravitational settling)} \\
 & = - \frac{\partial}{\partial D_p} (I(D_p, x, t)n(D_p, x, t)) \text{ (cond./evap.)} \\
 & + \frac{D_p^2}{2} \int_0^\infty \frac{\beta((D_p^3 - D_p'^3), D_p', x, t)}{(D_p^3 - D_p'^3)^{2/3}} \\
 & \times n((D_p^3 - D_p'^3)^{1/3}, x, t)n(D_p', x, t) dD_p' \text{ (coag. in)} \\
 & - n(D_p, x, t) \int_0^\infty \beta(D_p, D_p', x, t) \\
 & n(D_p', x, t) dD_p' \text{ (coag. out)} \\
 & + \nabla \cdot (\mathbf{K}(x, t)\nabla n(D_p, x, t)) \text{ (spatial diffusion)} \\
 & + N(D_p, x, t) \text{ (nucleation)} \\
 & + E(D_p, x, t) \text{ (emission)} \\
 & + R(D_p, x, t) \text{ (chemical reaction)}, \quad (1)
 \end{aligned}$$

where  $n(D_p, x, t)$  is the number distribution such that  $n(D_p, x, t) dD_p$  is the number concentration of particles in the range  $[D_p, D_p + dD_p]$ ,  $I(D_p, x, t)$  is the rate of change of particle diameter,  $dD_p/dt$ , due to condensation and evaporation.  $\beta(D_p, D_p')$  is the coagulation coefficient for particles with diameter  $D_p$  and  $D_p'$ ,  $x$  is the spatial coordinate vector;  $t$  is time;  $\mathbf{V}$  is the wind velocity vector,  $V_s$  is the settling velocity,  $k$  is the unit vector in the vertical direction,  $\mathbf{K}(x, t)$  is the turbulent diffusivity tensor;  $N$ ,  $E$  and  $R$  are, respectively, the nucleation, emission and reaction rate of particles in the range  $[D_p, D_p + dD_p]$ .

In the present paper, we restrict our attention to typical urban and regional atmospheric conditions, which include neither conditions of high r.h. like those in fog or cloud droplets, where aqueous-phase reactions (Kerminen and Wexler, 1995b) and turbulence-induced coagulation may influence the distribution (Wang et al., 2000), nor conditions very close to emission sources, where turbulent mixing and dilution may be significant.

## 3. Important physico-chemical processes: term-by-term analysis of Eq. (1)

Since there are so many processes happening in the atmosphere, we begin by analyzing each term in Eq. (1). Two cases could arise: (1) a process is too slow compared to other ones for part of or the whole size range we are concerned, (2) a process may be very fast, but its effects on the number distribution is insignificant if a small number of particles are formed or removed. So when either of these happens, the process is eliminated from the governing equation to increase computational and numerical efficiencies.

### 3.1. Condensation and evaporation

The condensation/evaporation term in Eq. (1) can be written as

$$\begin{aligned}
 & - \frac{\partial}{\partial D_p} (I(D_p, x, t)n(D_p, x, t)) \\
 & = \left( - \frac{\partial I}{\partial D_p} n \right) + \left( - \frac{\partial n}{\partial D_p} I \right). \quad (2)
 \end{aligned}$$

Condensation and evaporation do not change the total number of particles in an aerosol population, but they may alter the distribution. In this study, we call a change in the vertical position (upwards or downwards) of distribution curve 'growth', while in the horizontal position 'shift', shown in Fig. 1(a).

The first term on the right-hand side of Eq. (2) is the 'growth' term, which is caused by a gradient in  $I$  over  $D_p$ ,  $\partial I/\partial D_p \neq 0$ . If this gradient is zero, the height of the distribution does not change. Suppose that diameters of small particles grow faster by condensation than larger ones, which will be investigated in detail later this section, then the large particles cannot maintain the shifting speed of small ones, so the curve base becomes narrower, as shown in Fig. 1(b). Consequently, the curve moves upward so that the total area, in other words, the total number of particles, is conserved. This is the reason that condensation and evaporation leads to 'growth'.

The second term on the right-hand side of Eq. (2) represents the 'shift' in the distribution due to condensation and evaporation. As condensation proceeds, the particle diameter becomes larger and the distribution 'shifts' to the right. In case of evaporation, the curve 'shifts' to the left.

Let us now examine the relevance of condensation and evaporation to the number distribution by employing time scale analysis, where the time scale for 'growth' is  $\tau_g$ , and for 'shift' is  $\tau_s$ .

$$\tau_g^{-1} = \frac{1}{n} \left| - \frac{\partial I}{\partial D_p} n \right| = \left| - \frac{\partial}{\partial D_p} \left( \frac{dD_p}{dt} \right) \right|, \quad (3)$$

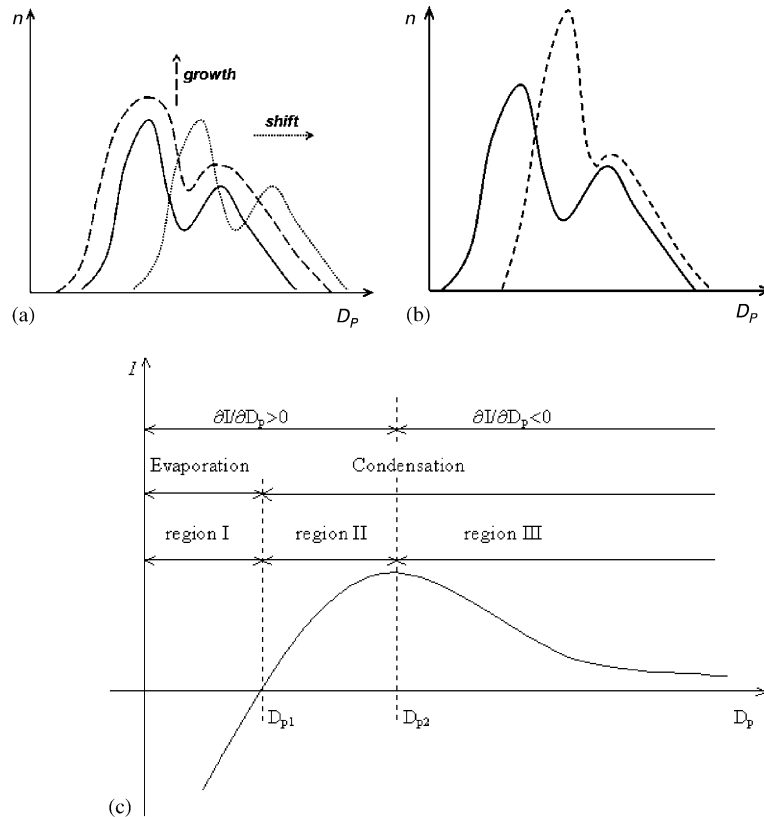


Fig. 1. (a) Demonstration of ‘growth’ (dashed line) and ‘shift’ (dotted line) in aerosol size distribution. (b) Development of growth and shift terms in aerosol number distribution. The solid lines represent the original distributions in both (a) and (b). (c) A sketch of ‘three regions’ for growth rate  $I$  vs. particle diameter  $D_p$  curve.

$$\begin{aligned} \tau_s^{-1} &= \frac{1}{n} \left| -\frac{\partial n}{\partial D_p} I \right| = \left| -\frac{1}{n} \frac{\partial n}{\partial D_p} \frac{dD_p}{dt} \right| \\ &= \left| -\frac{D_p}{n} \frac{\partial n}{\partial D_p} \frac{1}{D_p} \frac{dD_p}{dt} \right| \\ &= \left| -\frac{\partial \ln n}{\partial \ln D_p} \tau_G^{-1} \right|, \end{aligned} \quad (4)$$

where

$$\tau_G^{-1} = \frac{1}{D_p} \frac{dD_p}{dt},$$

$\tau_g$  is inversely proportional to the gradient in the condensation rate,  $I$ . From (4), we can see that  $\tau_s$  consists of two parts, one is the logarithmic slope of the distribution curve,  $\partial \ln n / \partial \ln D_p$ , describing its shape; the other is  $\tau_G$ , defined as a growth time scale due to condensation and evaporation (Kerminen and Wexler, 1995b). Since the slope is highly variable and also a function of  $n$  and  $D_p$ , we will focus our attention on  $\tau_G$ , which characterizes the magnitude of  $\tau_s$ .

The condensational mass flux of species  $i$  onto a single particle can be written as

$$\frac{dm_i}{dt} = \frac{2\pi D_i D_p [C_{i,\infty} - C_{i,\text{surf}}(D_p)]}{1 + \gamma_{c,i}(D_p, \alpha_i)}, \quad (5)$$

where  $m_i$  is the mass of species  $i$  in an individual particle of total mass  $m = \sum_{i=1}^s m_i$ ,  $D_i$  ( $\text{m}^2 \text{s}^{-1}$ ) is the gas-phase diffusion coefficient of species  $i$ , and  $C_i$  and  $C_{i,\text{surf}}$  ( $\text{kg m}^{-3}$ ) are its mass concentrations in the gas phase and over the particle surface, respectively. The factor  $\gamma_{c,i}$  accounts for the non-continuum effects and the imperfect accommodation of the condensate on the particle surface, the latter of which is described by the accommodation coefficient,  $\alpha_i$ . For most purposes, a sufficient approximation is  $\gamma_{c,i} = 2D_i / \alpha_i c_i D_p \approx 2\lambda / \alpha_i D_p$  (Wexler and Seinfeld, 1990), where  $c_i$  is the mean thermal molecular velocity of species  $i$  in air, and  $\lambda$  is the air mean free path. Since

$$I = \frac{dD_p}{dt} \approx \frac{2}{\pi \rho_p D_p^2} \frac{dm}{dt} \quad (6)$$

combining (5) and (6), we have

$$I = \sum_{i=1}^s \frac{4D_i}{D_p(1 + \gamma_{c,i}(D_p, \alpha_i))} \times \frac{[C_{i,\infty} - C_{i,\text{surf}}(D_p)]}{\rho_p} \quad (7)$$

The surface accommodation coefficient,  $\alpha$ , is the fraction of condensing molecules that stick upon colliding with the particle surface. In recent years, a better understanding of accommodation has been achieved. Dassios and Pandis (1999) showed that the processes of evaporation of ammonium nitrate aerosol particles can be described by using a temperature dependent accommodation coefficient varying from 0.8 to 0.5 in the temperature range 293–300 K. The results are in quantitative agreement with the suggestion of Clements et al. (1996), based on theoretical arguments, that general values of sticking coefficients can differ somewhat from unity but it should not be much less than this in conditions and processes having atmospheric relevance. So for our work a uniform accommodation coefficient,  $\alpha$ , for all species of 0.6 is assumed. Then we obtain a simplified form of (5):

$$I = \frac{1}{D_p(1 + 2\lambda/\alpha D_p)} \times \sum_{i=1}^s \frac{4D_i[C_{i,\infty} - C_{i,\text{surf}}(D_p)]}{\rho_p} \quad (8)$$

From (8), we can see the growth rate,  $I$ , can be either positive or negative, depending on the relative magnitudes of ambient as well as particle surface concentrations. The particle surface concentration,  $C_{i,\text{surf}}$ , is a function of  $D_p$  due to the Kelvin effect. The Kelvin effect serves to increase the equilibrium partial pressure over the particle by a factor of  $\exp(4\sigma v/\text{RTD}_p)$ , where  $\sigma$  is the surface tension and  $v$  is the molar volume of the species. Then a more detailed form of (8) is

$$I = \frac{1}{D_p(1 + 2\lambda/\alpha D_p)} \times \sum_{i=1}^s \frac{4D_i[C_{i,\infty} - C_{i,\text{surf}0} \exp(4\sigma_i v_i/\text{RTD}_p)]}{\rho_p} \quad (9)$$

The factor  $\exp(4\sigma v/\text{RTD}_p)$  is very big for small particles and damps exponentially to unity as particles become larger, which means that volatile gases tend to evaporate from the surfaces of small particles and condense on larger ones. So in many circumstances there exists a critical particle size, across which the growth rate,  $I$ , changes from negative to positive. This critical size will hereinafter be called  $D_{p1}$ .

Assuming uniform density, differentiate (9) with respect to  $D_p$  to obtain

$$\begin{aligned} \frac{\partial I}{\partial D_p} = & - \frac{1}{D_p^2(1 + 2\lambda/\alpha D_p)^2} \\ & \times \sum_{i=1}^s \frac{4D_i[C_{i,\infty} - C_{i,\text{surf}0} \exp(4\sigma v/\text{RTD}_p)]}{\rho_p} \\ & + \frac{1}{D_p(1 + 2\lambda/\alpha D_p)} \sum_{i=1}^s \frac{4D_i C_{i,\text{surf}0}}{\rho_p} \\ & \times \exp\left(\frac{4\sigma v}{\text{RTD}_p}\right) \frac{4\sigma v}{\text{RTD}_p} \frac{1}{D_p} \\ = & A + B. \end{aligned} \quad (10)$$

We call the first term on the left-hand side term  $A$  and second  $B$ . Term  $A$  can also be either positive or negative in the same manner as  $I$ .  $B$  is always positive, representing the changing of the Kelvin effect factor with respect to  $D_p$ , and its value decreases as particles become larger. Therefore there exists another critical size,  $D_{p2}$ , across which the gradient of  $I$  with respect to  $D_p$ ,  $\partial I/\partial D_p$ , changes from positive to negative. It is not difficult to prove that  $D_{p1}$  is always less than  $D_{p2}$ . A sketch of the  $I$  vs.  $D_p$  shows three regions divided by the two critical sizes,  $D_{p1}$  and  $D_{p2}$ , as shown in Fig. 1(c).

Next, we will investigate the growth rates in these regions. In region I, the negative growth rate and positive gradient mean that these particles tend to shrink, which is a shift to the left in Fig. 1(a), and the smaller particles shrink faster than larger ones. In region II, the growth rate is positive and its gradient over  $D_p$  is also positive. This part of the curve shifts to the right due to condensation and small particles shift slower than the larger ones. Hence the shift time scale,  $\tau_s$ , tends to infinity at  $D_{p1}$  and this curve shifts in the two opposite directions on the opposite sides of  $D_{p1}$ , which gives rise to our first ‘valley’ in the distribution. In region III, the growth rate is positive but its gradient is negative, which means that the curve shifts to the right and smaller particles shift faster than larger ones.

An interesting phenomenon happens around  $D_{p2}$ . At  $D_{p2}$ , the growth rate,  $I$ , is a maximum. Mathematically the gradient of the growth rate over  $D_p$  is zero at  $D_{p2}$ , which means that  $\tau_g$  in Eq. (3) is almost infinity. From Eq. (4) we can see that  $\tau_G$  is very small (but not necessarily a minimum). Recall that  $\tau_g$  is the time scale for ‘growth’ and  $\tau_G$  characterizes the magnitude of the time scale for ‘shift’,  $\tau_s$ . Then the scenario is that particles shift rapidly out of this size to larger ones because  $\tau_G$  is small, but the distribution does not grow very much because  $\tau_g$  is large. Here again, a valley in the distribution is anticipated. The whole process is dynamic. However, mathematically  $\tau_s$  goes to infinity when the slope of the distribution curve becomes zero. So once the ‘valley’ comes into shape, it tends to stay in rather fixed position.

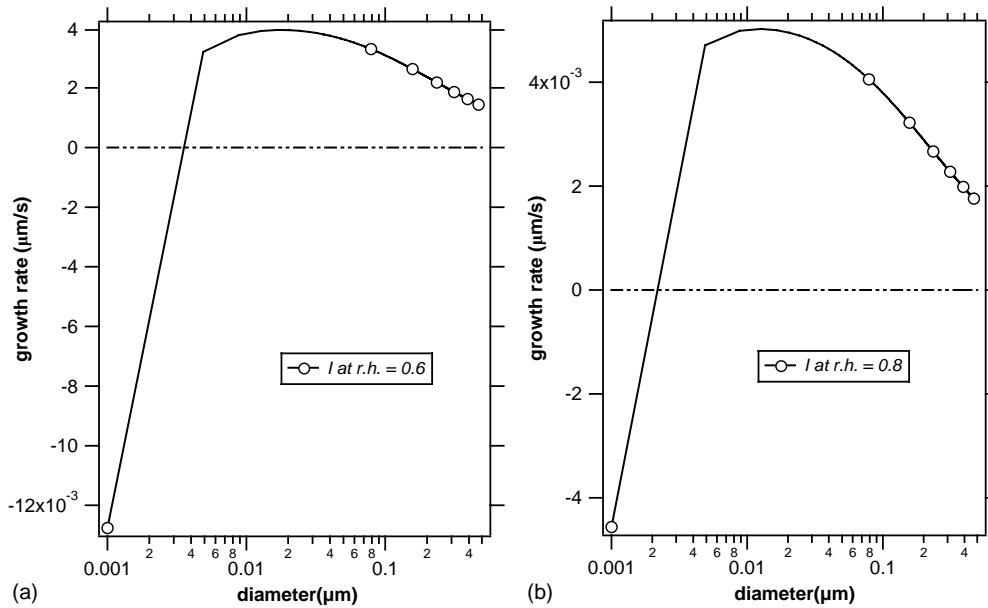


Fig. 2. Growth rate as a function of diameter at r.h. = 0.6 (a) and 0.8 (b).

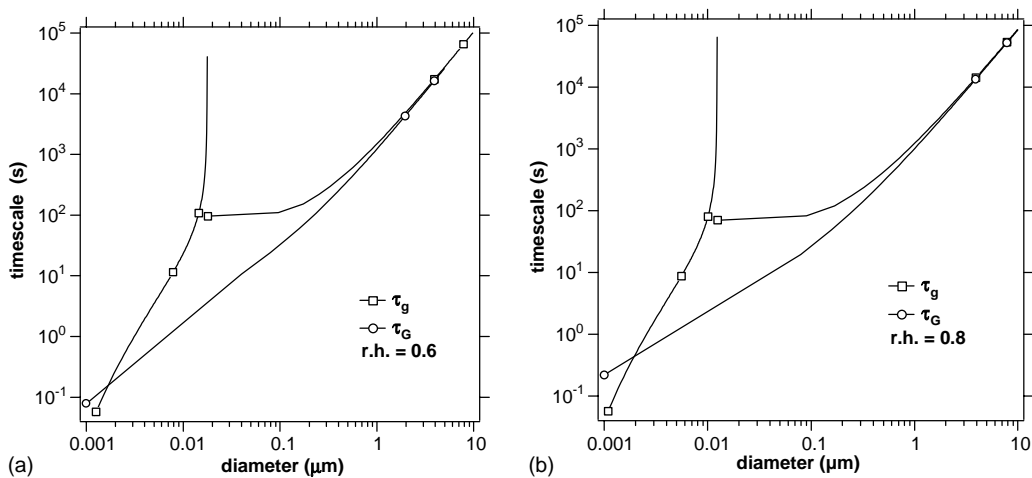


Fig. 3. Time scale for 'growth',  $\tau_g$ , and time scale for 'shift',  $\tau_G$ , vs. diameter at r.h. = 0.6 (a) and 0.8 (b).

The values of  $D_{p1}$  and  $D_{p2}$  depend on many factors, such as particle population, composition and relative humidity. Let us evaluate their approximate values as well as the two time scales under typical urban atmospheric conditions, which we take to be 30 and  $10 \mu\text{m}^{-3}$  for ammonia and nitric acid, respectively (Meng and Seinfeld, 1996). Since currently we have very little information on volatile organic compounds (VOC), so let us focus on the inorganics at this time, which influences will be discussed later in this section. To further simplify calculation,  $\sigma$  is taken the same value as water.

Using Eq. (9), the growth rates as a function of diameter at r.h. = 0.6 and 0.8, are plotted in Fig. 2(a) and (b), respectively, and they demonstrate the shape that we anticipated qualitatively in Fig. 1(c).  $D_{p1}$  in Fig. 2(a) is around 3.3 nm and in Fig. 2(b) 2.1 nm.  $D_{p2}$  in Fig. 2(a) is about 18 nm and in Fig. 2(b) 12 nm. The time scales vs. diameter curves at two different r.h. are plotted in Fig. 3. The singularity at  $D_{p2}$  is obvious.

The Kelvin effect plays a central role in condensation that shapes the particle number distribution for sizes in regions I and II. When are particles large enough that the Kelvin effect influence on condensation can be

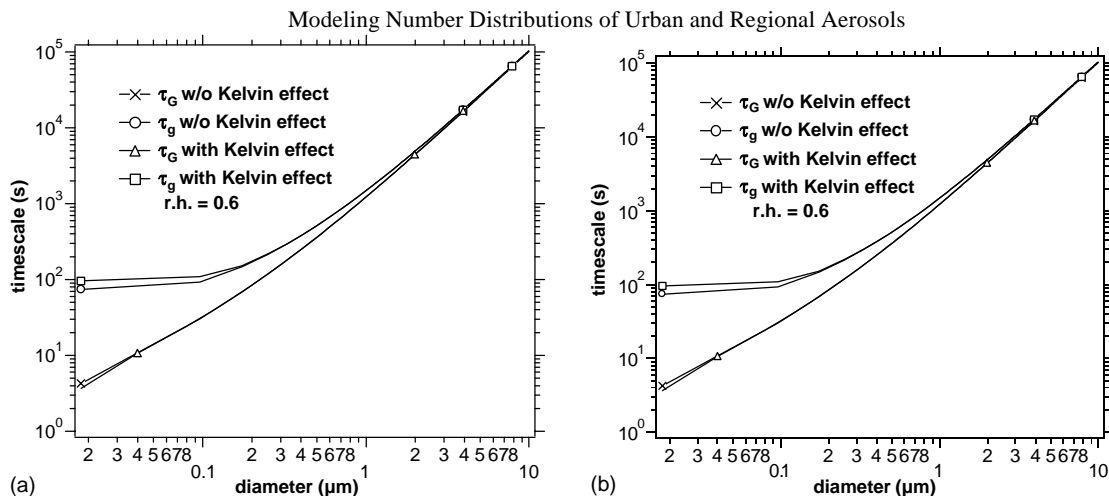


Fig. 4. Comparison between time scales computed with and without the Kelvin effect at r.h. = 0.6 (a) and 0.8 (b).

ignored? To answer this question, we plot region III of Fig. 3 with and without the Kelvin effect as Fig. 4.

So we can see that the timescale values of for two cases are close to each other in region III. Given the uncertain nature of atmospheric conditions, we choose  $0.05\ \mu\text{m}$  as the cutting point for the Kelvin effect computation, i.e., it is neglected for particles larger than this size.

Over what size range is condensation important? Fig. 4 shows that while  $\tau_g$  tends to be larger than  $\tau_G$  for small particles,  $D_p \ll 1\ \mu\text{m}$ , they are quite close to each other in the large particle limit,  $D_p \gg 2\ \mu\text{m}$ . We also found that both timescales are in the magnitude of  $10^1$ – $10^3$  s for a broad size range (from about  $0.01$ – $2\ \mu\text{m}$ ), fast enough to compare with other relevant timescales. So condensation and evaporation are important for the number distribution and should be considered in our model except for particles greater than about  $2\ \mu\text{m}$ .

The volatile organics were not considered in the time scale calculations. The influences of VOCs are twofold: on one hand, VOCs tend to condensate on existing particles, making related time scales smaller, i.e., the particle grow faster; on the other hand, organic coating on a particle surface may reduce the condensation of inorganic gases, then making time scales bigger. Considering that accommodation coefficients do not differ significantly from unity, the total effect is to decrease the growth time scales.

To summarize this section, the particle size domain can be divided into three regions. For particles smaller than about  $0.05\ \mu\text{m}$ , the Kelvin effect plays a significant role in condensation and evaporation. Particles larger than about  $2\ \mu\text{m}$  are not affected significantly by condensation and evaporation.

### 3.2. Coagulation

Coagulation has been shown to be negligible for mass distributions (Wexler et al., 1994). Here we investigate its effects on number distributions.

#### 3.2.1. Brownian coagulation

Two physically different cases will be examined here: intermodal coagulation and intramodal coagulation.

Coagulation of small particles with large ones will not change the number of large particles, but will reduce the number of small particles. In addition, coagulation onto large particles is similar to condensation in that it may result in significant 'growth' and 'shift'. The diameter of a new particle,  $D_n$ , after small particles with diameter  $D_s$  coagulating with large particles with diameter  $D_l$ , is roughly  $D_n = \sqrt[3]{D_s^3 + D_l^3}$ . The particles of interest in our work have a range of diameters from about  $0.001$ – $10\ \mu\text{m}$ . With five orders of magnitude spanned,  $D_l^3 \gg D_s^3$ , so small particles coagulating with large ones will not substantially alter the diameter of the larger particles, which means the shifting speeds are very slow. We already know that 'growth' term is caused by gradients in shifting speeds. Since the larger particles have similar or comparable diameters and all shift very slowly, the differences in shifting speeds will not be large. Thus, this 'growth' term can be neglected and coagulation does not significantly affect the size distribution of large particles. With this in mind, we assess the importance of intermodal coagulation by identifying and evaluating  $\tau_{\text{coag}}$ , the time scale for depletion of small particles due to coagulation with large ones.

The time scale for depletion of the number of small particles due to Brownian coagulation,  $\tau_{\text{coag}}$ , is  $\tau_{\text{coag}} = |n^s / (dn^s / dt)|$ , which is equal to  $|m^s / (dm^s / dt)|$ , the same

as the time scale for depletion of mass of small particles (Wexler et al., 1994). Thus,  $\tau_{\text{coag}}$  can be approximated by

$$\tau_{\text{coag}} = \frac{1}{2\pi D_s \hat{\beta} \hat{D}_{\text{pl}} \hat{n}} = \frac{\hat{D}_{\text{pl}}^2 \rho_p}{12 D_s \hat{\beta} \hat{m}_p}, \quad (11)$$

where  $\hat{D}_{\text{pl}}$  and  $\hat{n}$  are the equivalent mono-disperse diameter and number of the larger particle,  $\hat{\beta}$  is the equivalent non-continuum correction factor, and  $\hat{m}_p$  is the large particle mass loading (Wexler et al., 1994). But, is coagulation important? We answer this by comparing coagulation to the competing processes, i.e., condensation and deposition. As we did in the previous section, the comparisons will be made in the three regions of Fig. 1(c), respectively.

As we have discussed earlier, condensation on particles in region I is inhibited by the Kelvin effect, limiting growth rate, which in turn causes increased diffusivity. Large diffusivities promote coagulation, but the deposition velocity will also become larger. Therefore, we must compare the time scales between deposition of small particles and their coagulation on large ones. The deposition time constant is  $L/V_d$ , where  $L$  is the inversion height and of order of 1000 m or  $10^5$  cm and  $V_d$  is the deposition velocity, depending on the stability conditions, but with a value around  $1.0 \text{ cm s}^{-1}$ . Thus the deposition time constant is of the order of  $10^5$  s. How about coagulation? We choose  $D_{\text{pl}} = 0.3 \mu\text{m}$ , the geometric diameter of the large particles;  $m_p = 50 \mu\text{g m}^{-3}$ , the mass loading of large particles;  $D_s = 5.8 \times 10^{-7} \text{ m}^2 \text{ s}^{-1}$ , the diffusivity of  $0.003 \mu\text{m}$  particles;  $\hat{\beta} = 0.07$ , the non-continuum correction for coagulation of  $0.003 \mu\text{m}$  particles on  $0.3 \mu\text{m}$  ones;  $\rho_p = 10^3 \text{ kg m}^{-3}$ , the minimum density. We get  $\tau_{\text{coag}}$  roughly 370 s, which means these extremely tiny nuclei are subject to scavenging by preexisting particles and their surface depositions can be neglected.

In regions II and III, volatile gases readily condense on particles to make them grow. When particles grow larger, their diffusivities decrease, and so do the coagulation rates, i.e., condensation may suppress coagulation. Do small particles grow so fast that the effects of coagulation become insignificant? Define a time scale  $\tau_{\text{c,g}}$ , over which the coagulation rate changes due to particle growth. Since the rate at which small particles coagulate with larger ones is proportional to the small particle diffusivity,  $D_s$ ,  $\tau_{\text{c,g}}$  can be estimated from

$$\tau_{\text{c,g}}^{-1} = \frac{1}{D_s} \left| \frac{dD_s}{dt} \right| \approx \frac{2}{D_p} \left| \frac{dD_p}{dt} \right|, \quad (12)$$

where the latter equality is due to the proportionality of diffusivity to  $D_p^2$  for small particles (Kerminen and Wexler, 1995a). Thus  $\tau_{\text{c,g}}$  has the same magnitude as  $\tau_G$ , the growth time scale by condensation,  $\tau_{\text{c,g}} \cong \tau_G$ . So if  $\tau_{\text{c,g}}$  is bigger than or the same magnitude as  $\tau_{\text{coag}}$ , small particles coagulate before they grow too large and

coagulation is important. Otherwise, coagulation can be ignored.

We have already shown that  $\tau_G$  has a magnitude of  $10^1$ – $10^3$  s (see Fig. 3), so what mass loading would give significant coagulation? Let  $\tau_{\text{coag}}$  equal  $10^3$  s and choose the same set of data for large particles as above and  $D_s = 5.24 \times 10^{-8} \text{ m}^2 \text{ s}^{-1}$ , the diffusivity of  $0.01 \mu\text{m}$  particles, Assuming  $\hat{\beta} = 0.86$ , the non-continuum correction for coagulation of  $0.01 \mu\text{m}$  particles on  $0.3 \mu\text{m}$  ones, we obtain a rather conservative value of  $\hat{m}_p$  over  $170 \mu\text{g m}^{-3}$ , about three to five times larger than typical mass loadings. So coagulation can hardly occur before condensation grows particles too large to efficiently coagulate.

Up to now we are mainly dealing with the effects of coagulation on either very small particles or very large ones. To extend our study to the whole size range, we simulated coagulation for a typical urban aerosol size distribution given by Jaenicke (1993), which also appears in Seinfeld and Pandis (1998) as Table 7.3. We found that particles tend to coagulate on particles larger than about  $0.05 \mu\text{m}$  and that particles larger than about  $0.05 \mu\text{m}$  do not coagulate onto even larger ones. The coagulation growth time scales,  $\tau_{\text{G,coag}}$ , was evaluated to investigate whether the particle growth by coagulation can significantly alter the number distributions. For a discrete distribution,  $\tau_{\text{G,coag}}$  has the form of

$$\tau_{\text{G,coag}}^{-1} = \frac{1}{D_{\text{pi}}} \frac{dD_{\text{pi}}}{dt} = \frac{\sum_{i>j} K_{ij} N_j D_{\text{pj}}^3}{3 D_{\text{pi}}^3}, \quad (13)$$

where  $D_{\text{pi}}$ ,  $N_i$ ,  $D_{\text{pj}}$  and  $N_j$  are mean diameters and number concentrations for bin  $i$  and  $j$ , respectively, and  $K_{ij}$  is the coagulation coefficient for particles in bin  $i$  coagulating with those in bin  $j$ . The numerical results of  $\tau_{\text{G,coag}}$  were illustrated in Fig. 5. Since  $\tau_{\text{G,coag}}$  has the range from  $10^5$  to  $10^9$  s, coagulation is not an efficient mechanism for particle growth under typical urban conditions.

Intramodal coagulation may also alter the number distributions of particles. The time scale for this kind of coagulation is  $\tau_{\text{s,coag}} = 2/K_{i,j} \hat{n}$ . The intramodal coagulation coefficient is relatively independent of particle size and has the magnitude of  $10^{-9} \text{ cm}^3 \text{ s}^{-1}$ . So in order to have a time constant around  $10^3$  s, the equivalent mono-disperse particle number concentration has to be as high as  $10^6 \text{ cm}^{-3}$ . Such high number concentrations rarely happen even for ultrafine particles in the atmosphere (Shi and Harrison, 1999; Morawska et al., 1999; Buzorius et al., 1999; Hughes et al., 1998). So intramodal coagulation can hardly be important for number distributions except in the case of the extremely high number concentration, such as near emissions or just after a nucleation event.

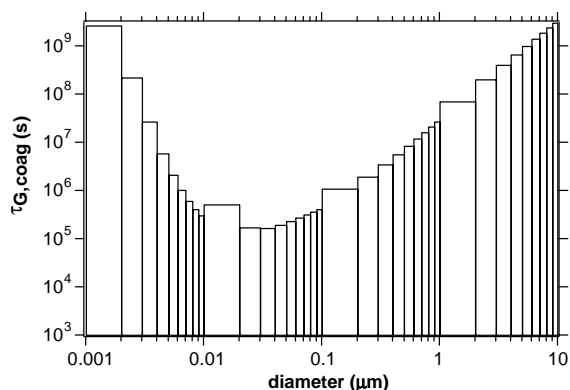


Fig. 5. Coagulation growth time scale for a typical urban aerosol number distribution.

### 3.2.2. Gravitational settling and turbulent shear

Coagulation settling may cause coagulation because of the differential settling velocity of large and small particles. The coagulation coefficient is proportional to the products of the target area and the relative distance swept out by the larger particles per unit time,  $K_{12}^{GS} = \pi D_{pl}^2/4(v_{tl} - v_{ts})$ ,  $D_{pl} \gg D_{ps}$ , where  $v_{tl}$  and  $v_{ts}$  are the terminal settling velocities for the larger and small particles, respectively. The time scale for coagulation due to gravitational settling is

$$\tau_{gs} = 2\hat{D}_{pl}\rho_p/3\hat{V}_t\hat{m}_p \quad (14)$$

and is too slow to have a significant influence on the size distribution (Wexler et al., 1994).

The analysis of Saffman and Turner (1956) gives the coagulation coefficient due to turbulent shear as

$$K_{12}^{TS} = \left(\frac{\pi\varepsilon_k}{120\nu}\right)^{1/2} (D_{pl} + D_{ps})^3, \quad (15)$$

where  $\sqrt{\varepsilon_k/\nu}$  is the characteristic turbulent shear rate at the length scales relevant to particle coagulation. The time scale for turbulent shear coagulation is  $\tau_{ts} = \rho_p/(48\hat{m}_p\sqrt{\varepsilon_k/120\nu})$  (Wexler et al., 1994). It should be noted that the above expression was derived for finite-size particles with zero inertia in isotropic turbulence (Wang et al., 1998), which may not always apply in the atmosphere and therefore worthy of further discussion. Zero inertia means that the particle follow the local fluid motion precisely, which translates into the particle inertial response time scale,  $\tau_p = \rho_p D_p^2/(18\rho\nu)$ , being much smaller than the flow Kolmogorov time scale,  $\tau_K = (\nu/\varepsilon_k)^{1/2}$ , where  $\rho_p$  and  $\rho$  are the particle and fluid density;  $\nu$  and  $\varepsilon_k$  are fluid kinematic viscosity and average rate of energy dissipation per unit mass. We choose  $\rho_p$  as  $1.4 \times 10^3 \text{ kg m}^{-3}$ ,  $\rho = 1.2 \text{ kg m}^{-3}$  and  $\nu = 1.5 \times 10^{-5} \text{ m}^2 \text{ s}^{-1}$  to obtain  $\tau_p$  around  $10^{-8}$ – $10^{-7}$  s for  $0.1 \mu\text{m}$  particles and  $10^{-4}$ – $10^{-3}$  s for  $10 \mu\text{m}$  ones.  $\tau_K$

is determined by  $\varepsilon_k$ , which could have a wide range from  $10$  to  $10^3 \text{ cm}^2 \text{ s}^{-3}$ , depending on the metrological conditions. But under typical urban conditions,  $\tau_K$  has the order of  $10^{-2}$ – $10^{-1}$  s. So generally speaking  $\tau_p$  is much less than  $\tau_K$  for the particles within the size range of concern in this study. However, the zero-inertia approximation may not apply in clouds, where droplets could be as large as  $250 \mu\text{m}$  and dissipation rates up to  $2500 \text{ cm}^2 \text{ s}^{-3}$  in very strong cumulus congestus. The corresponding effects can lead to  $10^2$ – $10^3$  times increase in the collision rate. This may help explain the rapid growth of droplets in the size ranges where neither condensation nor differential gravitational settling is effective (Wang et al., 2000).

We found that time constants for both settling and turbulent shear are the same for mass and number distributions. So using the same reasoning as that in Wexler et al. (1994), the coagulation due to gravitational settling and turbulent shear can be neglected, except for very intense turbulence that may occur in clouds. As mentioned previously in this work, we are only considering atmospheric conditions outside of cloud so turbulent coagulation can be ignored.

In summary, coagulation is inefficient for particle growth under typical urban conditions; intermodal Brownian coagulation may be important for the number distribution of sufficiently small particles, and will be simulated for particles smaller than  $0.05 \mu\text{m}$ .

### 3.3. Gravitational settling

Gravitational settling may affect deposition to the surface and the vertical distribution of particles in the atmosphere.

#### 3.3.1. Compared to dry deposition

Gravitational settling substantially influences surface deposition if the settling velocity,  $V_s$ , is significant compared to the deposition velocity,  $V_d$ . For particle diameters much greater than the mean free path of air, the settling velocity is given by

$$V_s = \frac{D_p^2 \rho_p g}{18\mu}, \quad (16)$$

where  $D_p$  is the particle diameter,  $\rho$  is its density,  $g = 9.8 \text{ m s}^{-2}$  is the gravitational constant, and  $\mu$  is the viscosity of air. The deposition velocity is

$$V_d = \frac{1}{r_a + r_b + r_a r_b V_s} + V_s, \quad (17)$$

where  $r_a$  is the aerodynamic resistance and  $r_b$  the quasi-laminar layer resistance.

In the absence of settling,  $V'_d = 1/(r_a + r_b)$ . We assume that particle settling may affect deposition when

$V_s > V'_d/10$ , which gives

$$D_p \geq \sqrt{\frac{2\mu}{\rho_p g(r_a + r_b)}} \quad (18)$$

So the larger ( $r_a + r_b$ ), the more important settling is.

The absolute magnitude of  $r_b$  does not change significantly over stability conditions, but the magnitude of  $r_a$  does. Here we choose  $r_a$  as  $150 \text{ s m}^{-1}$ , a rather conservatively large value, and try to obtain the lower limit of  $D_p$ . Fig. 6 depicts the comparison between  $V'_d$  and gravitational settling velocity. We can see that settling velocity becomes important when particles are larger than about  $1 \mu\text{m}$ . So we need to keep gravitational settling term in dry deposition.

### 3.3.2. Compared to vertical turbulent diffusion

Vertical transport of aerosol particles is governed by turbulent diffusion, advection and gravitational settling. It is expected that for the smallest particles settling will be negligible compared to vertical turbulent diffusion, but for particles sufficiently large it will be significant. Wexler et al. (1994) showed that under unstable atmospheric conditions particles less than about  $20 \mu\text{m}$  are not significantly affected by settling compared to turbulent diffusion and under nighttime conditions, the atmosphere is stably stratified or neutral with a turbulent diffusivity greater than only  $1 \text{ m}^2 \text{ s}^{-1}$ , so particles less than about  $4 \mu\text{m}$  are not significantly affected by settling.

In summary, we found gravitational settling significantly affect particle dry deposition. Using the similar reasoning as that in Wexler et al. (1994), it is not important to turbulent transport. As a consequence, gravitational settling is neglected for turbulent transport, but retained for deposition calculations.

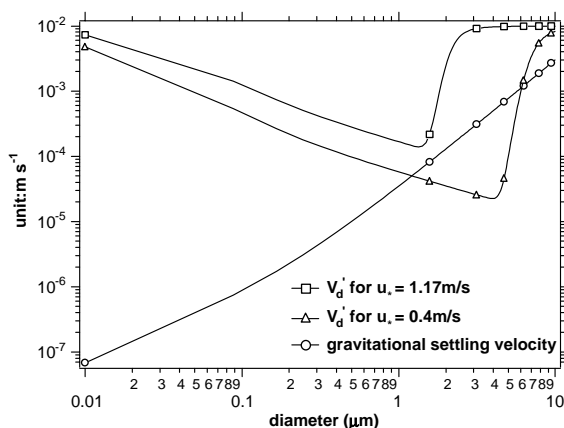


Fig. 6. Comparison between  $V'_d$  and settling velocity.

### 3.4. Nucleation

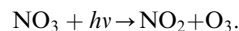
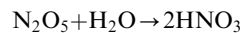
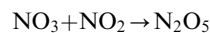
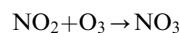
Wexler et al. (1994) has shown that  $\text{H}_2\text{SO}_4\text{-H}_2\text{O}$  or  $\text{H}_2\text{SO}_4\text{-NH}_3\text{-H}_2\text{O}$  nucleation (Eisele and McMurry, 1997) may form new particles under conditions of low aerosol loading and high ambient  $\text{SO}_2(g)$  concentrations. With a concentration of  $2 \times 10^9 \text{ molecules cm}^{-3}$  and 80% r.h., the freshly nucleated particles are estimated to grow to  $0.01 \mu\text{m}$  in about 400 s, which is an order of magnitude faster than the condensation or deposition time scales. So the nuclei will not be substantially removed from the atmosphere before they grow to significant size. In summary, nucleation may have negligible effect on the mass distributions, but they can change the number distribution significantly.

### 3.5. Chemical reaction

Chemical reactions in the particle phase cannot form new particles, but may cause them to grow or shrink similar to condensation and evaporation. In Wexler et al. (1994), two reactions were considered for their effects on mass distributions. One is oxidation of  $\text{SO}_2$  to sulfuric acid; the other is reaction of  $\text{N}_2\text{O}_5$  with particulate water to form nitric acid.

$\text{SO}_2$  oxidation is limited by the available liquid water, so at the RH values considered here, the S(VI) production rate is insignificant.

Heterogeneous oxidation of  $\text{NO}_x$  via reaction culminates in hydrolysis of  $\text{N}_2\text{O}_5$  on aerosol surfaces. Photolysis reaction terminates this pathway (Jacob, 2000).



Due to the rapid photolysis of nitrate radical and reduction of  $\text{O}_3$  below the inversion by  $\text{NO}$  emissions at night,  $\text{N}_2\text{O}_5$  is expected to form at night and aloft, where heterogeneous reaction may be limited by low aerosol loading (Wexler et al., 1994). This qualitative argument was consistent with later study on nitrogen deposition at Harvard Forest at an elevation of 340 m, which shows heterogeneous production of  $\text{HNO}_3$  is efficient (Munger et al., 1998), and measurement of concentrations of  $\text{NO}_3$  and  $\text{NO}_2$  in the San Joaquin Valley, which shows homogenous gas-phase removal processes of  $\text{NO}_3$  and  $\text{N}_2\text{O}_5$  are faster than their heterogeneous counterparts (Smith et al., 1995). Heterogeneous formation of  $\text{HNO}_3$  from  $\text{N}_2\text{O}_5$  and  $\text{H}_2\text{O}$  is less important than homogenous processes under typical urban conditions, so is not considered. No other heterogeneous reaction processes

appear to cause significant particle growth so are neglected.

### 3.6. Emissions

Particulate emissions are very important to both number and mass size distributions. Here we investigate whether emissions are so important to number distributions that other physical processes may become negligible compared to it. The current study is very tentative, not just because emission rates are sharply different from a residential neighborhood to an urban freeway corridor, but emission rates in the form of number distribution are rare—currently most emission rates are given in term of mass.

To include all emission sources is beyond the scope of this work, so which sources influence ultrafine number concentrations significantly? A recent study (Booker, 1997) performed in urban and rural Oxfordshire showed that particle number concentrations are strongly correlated with vehicle traffic while  $\text{PM}_{10}$  was essentially uncorrelated with traffic, suggesting mobile sources account for most of the number emissions in urban areas.

What are the emission rates of mobile sources? Bagley et al. (1996) showed emission rates of 290,000 particles per  $\mu\text{m}^3$ -PM emitted with geometric number diameter of 0.011  $\mu\text{m}$  for new technology diesel engines. Kittelson (1998) suggested a range of 2600 particles per  $\mu\text{m}^3$ -PM emitted with a geometric number diameter of 0.043  $\mu\text{m}$  for diesel engines. The huge differences between these two studies may arise from their respective soluble organic fraction (SOF) values (Kittelson, 1998). If we assume particle density of  $1.0 \text{ g cm}^{-3}$  and average PM emission rate of  $5.0 \text{ mg mile}^{-1}$  (Durbin et al., 1999), the former is equivalent to around  $10^{15}$  particles  $\text{km}^{-1}$  and latter  $10^{13}$  particles  $\text{km}^{-1}$ . Rickeard et al. (1996) observed rates of about  $1 \times 10^{14}$  and  $1\text{--}2 \times 10^{14}$  particles  $\text{km}^{-1}$  for spark-ignition and light-duty diesel vehicles, respectively. Since the studies above were mainly on light-duty vehicles and heavy-duty vehicles usually have one to two magnitude higher emissions, we can expect an emission rate up to  $10^{16}$  particles  $\text{km}^{-1}$  for heavy-duty trucks. However, much lower emission rates were observed by Kirchstetter et al. (1999), suggesting the emission rates for heavy-duty diesel trucks and light-duty vehicles are  $6.3 \times 10^{12}$  and  $4.6 \times 10^{10}$  particles per kg fuel, respectively. If we assume fuel density of  $0.7 \text{ g cm}^{-3}$  and average fuel economy of  $8.6 \text{ km l}^{-1}$  (Singer and Harley, 2000), the emission rate is equal to about  $5.0 \times 10^{11}$  and  $3.0 \times 10^9$  particles  $\text{km}^{-1}$ . So there is a large uncertainty in the particulate number emission rate ranging from  $10^9$  to  $10^{14}$  for gasoline engine vehicles and from  $10^{10}$  to  $10^{16}$  particles  $\text{km}^{-1}$  for diesel engine vehicles. An average emission rate of  $10^{15}$  particles  $\text{km}^{-1}$  may be a possible upper limit, considering the balancing

facts that the majority of the motor fleet is made up of light-duty vehicles but the average is strongly influenced by high emission vehicles. Since most of the particle number emitted by engines is in the ultrafine particle range,  $D_p < 0.05 \mu\text{m}$  (Kittelson, 1998), we believe that the ultrafine particle emission rate is of similar magnitude of  $10^{15}$  particles  $\text{km}^{-1}$ .

How to compare emissions to other mechanisms? To answer this question,  $\tau_e$ , the emission time scale is introduced here. Since the number emission rates of mobile sources usually have units of particles per km, we multiply by  $V_i$ , the average speed, to have the emission rate in particles per second. Then  $\tau_e$  has the form of

$$\tau_e^{-1} = \frac{\sum N_i \cdot E_i \cdot V_i}{C \cdot A \cdot H}, \quad (19)$$

where  $E_i$  is the emission rates of source type  $i$  in term of particles per second,  $N_i$  is the average number of such sources in the studied area,  $C$  is the ambient number concentration (particles  $\text{m}^{-3}$ ),  $A$  is the study area, and  $H$  is the mixing height (km).

Using Eq. (19) to evaluate  $\tau_e$ , with  $N_i = 1280$  vehicles in an  $A = 2 \text{ km} \times 2 \text{ km}$  region (approximated by studying a 16 block by 16 block area in downtown Sacramento),  $E_i = 10^{15}$  particles  $\text{km}^{-1}$ ,  $V_i = 40 \text{ km h}^{-1}$ ,  $C = 10^4$  particles  $\text{cm}^{-3}$ , a typical ambient number concentration for ultrafine particles, and emission height of 1 km, we get  $\tau_e$  around 1280 s. However, we can see from Eq. (19) that  $\tau_e$  strongly depends on  $H$ , the mixing height, which could be as low as just above ground in early morning, when emissions reach the peak due to commute traffic. Under those conditions,  $\tau_e$  could be just 10 s or even smaller, fast enough to compete with any other process.

## 4. Conclusion

We have analyzed the different processes in the atmosphere and evaluated their importance to aerosol number distribution predictions. With a detailed mathematical description, the influence of the Kelvin effect on condensation and evaporation has been elucidated; it is shown that condensation and evaporation are important for number distribution and the Kelvin effect must be considered for particles  $< 0.05 \mu\text{m}$ ; the relationship of growth rate with respect to particle size is shown to have a ‘three-region’ pattern; coagulation is too slow to influence particle number distributions for particle diameters  $> 0.05 \mu\text{m}$ , where condensation is the leading process. For particles smaller than this, condensation and evaporation, coagulation, nucleation and emissions interact with each other under typical urban conditions; gravitational settling is shown to significantly affect particle dry deposition, but can be neglected for vertical turbulent transport; chemical reactions are negligible. It

should be noted that most of our studies are based on the daytime urban data. During the nighttime, photochemistry is cut off and emissions significantly decrease, which leads to lower concentrations of both volatile or condensable gases and particles. Thus time scales increase together and the relative importance of different mechanisms remains about the same.

### Acknowledgements

This work is supported by EPRI.

### References

- Bagley, S.T., Baumgard, K.J., Gratz, L.G., Johnson, J.H., Leddy, D.G., 1996. Characterization of fuel and after treatment device effects on diesel emissions. Health Effects Institute (HEI), Research Report No.76.
- Booker, D.R., 1997. Urban Pollution Monitoring: Oxford Study. AEA Technology, Harwell, England.
- Buzorius, G., Hameri, K., Pekkanen, J., Kulmala, M., 1999. Spatial variation of aerosol number concentration in Helsinki city. *Atmospheric Environment* 33 (4), 553–565.
- Clement, C.F., Kulmala, M., Velsala, T., 1996. Theoretical consideration of sticking probabilities. *Journal of Aerosol Science*. 27 (6), 869–882.
- Dassios, K.G., Pandis, S.N., 1999. The mass accommodation coefficient of ammonium nitrate aerosol. *Atmospheric Environment* 33 (18), 2993–3003.
- Durbin, T.D., Norbeck, J.M., Smith, M.R., Truex, T.J., 1999. Particulate emission rates from light-duty vehicles in South Coast Air Quality Management District. *Environmental Science and Technology* 33 (24), 4401–4406.
- Eisele, F.L., McMurry, P.H., 1997. Recent progress in understanding particle nucleation and growth. *Philosophical Transactions of the Royal Society of London Series B* 352 (1350), 191–200.
- Gelbard, F., Seinfeld, J.H., 1979. General dynamic equation for aerosols—theory and application to aerosol formation and growth. *Journal of Colloid and Interface Science* 68 (2), 363–382.
- Hughes, L.S., Cass, G.R., Gone, J., Ames, M., Olmez, I., 1998. Physical and chemical characterization of atmospheric ultrafine particles in the Los Angeles area. *Environmental Science and Technology* 32 (9), 3730–3736.
- Jacob, D.J., 2000. Heterogeneous chemistry and troposphere ozone. *Atmospheric Environment* 34 (12–14), 2131–2159.
- Jaenicke, R., 1993. In: Hobbs, P.V. (Ed.), *Troposphere Aerosols, in Aerosol-Cloud-Climate Interactions*. Academic Press, San Diego, CA.
- Kerminen, V.-M., Wexler, A.S., 1995a. The interdependence of aerosol processes and mixing in point source plumes. *Atmospheric Environment* 29 (3), 361–375.
- Kerminen, V.-M., Wexler, A.S., 1995b. Growth laws for atmospheric aerosol particles: an examination of the bimodality of the accumulation mode. *Atmospheric Environment* 29 (22), 3263–3275.
- Kirchstetter, T.W., Harley, R.A., Kreisberg, N.M., Stolzenburg, M.R., Hering, S.V., 1999. On-road measurement of fine particle and nitrogen oxide emissions from light- and heavy-duty motor vehicles. *Atmospheric Environment* 33 (18), 2955–2968.
- Kittelson, D.B., 1998. Engines and nanoparticles: a review. *Journal of Aerosol Science* 29 (5–6), 575–588.
- Meng, Z.Y., Seinfeld, J.H., 1996. Time scales to achieve atmospheric gas-aerosol equilibrium for volatile species. *Atmospheric Environment* 30 (16), 2889–2900.
- Morawska, L., Thomas, S., Gilbert, D., Greenaway, C., Rijnders, E., 1999. A study of the horizontal and vertical profile of submicrometer particles in relation to a busy road. *Atmospheric Environment* 33 (8), 1261–1274.
- Munger, J.M., Fan, S.M., Bakwin, P.S., Goulden, M.L., Goldstein, A.H., Colman, A.S., Wofsy, S.C., 1998. Regional budgets for nitrogen oxides from continental sources: variations of rates for oxidation and deposition with season and distance from source regions. *Journal of Geophysical Research* 103 (D7), 8355–8368.
- Oberdorster, G., 2001. Pulmonary, effects of inhaled ultrafine particles. *International Archives of Occupational and Environmental Health* 74 (1), 1–8.
- Peters, A., Wichmann, H.E., Tuch, T., Heinrich, J., Heyder, J., 1997. Respiratory effects are associated with the number of ultrafine particles. *American Journal of Respiratory and Critical Care Medicine* 155 (4), 1376–1383.
- Pilinis, C., 1990. Derivation and numerical solution of the species mass distribution equations for multicomponent particulate systems. *Atmospheric Environment* 24A (7), 1923–1928.
- Pilinis, C., Seinfeld, J.H., 1987a. Asymptotic solution of the aerosols general dynamic equation for small coagulation. *Journal of Colloid and Interface Science* 115 (2), 472–479.
- Pilinis, C., Seinfeld, J.H., 1987b. Continued development of a general equilibrium model for inorganic multicomponent atmospheric aerosols. *Atmospheric Environment* 21 (11), 2453–2466.
- Pilinis, C., Seinfeld, J.H., Seigneur, C., 1987. Mathematical modeling of the dynamics of multicomponent atmospheric aerosols. *Atmospheric Environment* 21 (4), 943–955.
- Rickeard, D.J., Bateman, J.R., Kwon, Y.K., McAughy, J.J., Dickens, C.J., 1996. Exhaust particulate size distributions: vehicle and fuel influences in light duty vehicles. SAE Paper No. 961980.
- Saffman, P.G., Turner, J.S., 1956. On the collision of drops in turbulent clouds. *Journal of Fluid Mechanics* 1, 16.
- Seinfeld, J.H., Pandis, S.N., 1998. *Atmospheric Chemistry and Physics: From Air Pollution to Climate Change*. Wiley, Inc., New York.
- Shi, J.P., Harrison, R.M., 1999. Investigation of ultrafine particle formation during diesel exhaust dilution. *Environmental Science and Technology* 33 (21), 3730–3736.
- Singer, B.C., Harley, R.A., 2000. A fuel-based inventory of motor vehicle exhaust emissions in the Los Angeles area during summer 1997. *Atmospheric Environment* 34 (11), 1783–1795.
- Smith, N., Plane, J.M.C., Nien, C.F., Solomon, P.A., 1995. Nighttime radical chemistry in the San Joaquin valley. *Atmospheric Environment* 29 (21), 2887–2897.

- Wang, L.-P., Wexler, A.S., Zhou, Y., 1998. On the collision rate of small particles in isotropic turbulence. 1. Zero-inertia case. *Physics of Fluids* 10 (1), 266–276.
- Wang, L.-P., Wexler, A.S., Zhou, Y., 2000. Statistical mechanical description and modeling of turbulent collision of inertial particles. *Journal of Fluid Mechanics* 415, 117–153.
- Wexler, A.S., Seinfeld, J.H., 1990. The distribution of ammonium salts among a size and composition dispersed aerosol. *Atmospheric Environment* 24A (5), 1231–1246.
- Wexler, A.S., Lurmann, F.W., Seinfeld, J.H., 1994. Modeling urban and regional aerosols—I. Model development. *Atmospheric Environment* 28 (3), 531–546.